J|A|C|S
ARTICLES
Published on Web 10/31/2002

Mechanistic Insights into the Pd(BINAP)-Catalyzed Amination of Aryl Bromides: Kinetic Studies under Synthetically Relevant Conditions

Utpal K. Singh,[†] Eric R. Strieter,[†] Donna G. Blackmond,*[,‡] and Stephen L. Buchwald*[,†]

Contribution from the Department of Chemistry, Massachusetts Institute of Technology, Cambridge, Massachusetts 02139 and Department of Chemistry, University of Hull, Hull, HU6 7RX, U.K.

Received May 13, 2002

Abstract: Kinetic studies using reaction calorimetry were carried out under synthetically relevant conditions to study the mechanism of the amination of bromobenzene with primary and secondary amines using $Pd_2(dba)_3$/BINAP mixtures as well as preformed (dba)Pd(BINAP), (*p*-tolyl)(Br)Pd(BINAP), and $Pd(BINAP)_2$ complexes. The presence of a significant induction period in the reaction was attributed to the slow activation of the catalytic precursor, resulting in an increase in the concentration of active species within the catalytic cycle. The induction period can mask the true kinetics of the reaction, which exhibits positive order dependences on aryl bromide and amine and zero-order dependence on base. It is also determined that the bis-ligand complex $Pd(BINAP)_2$ does not play a role directly on the catalytic cycle. In addition to the conventionally accepted pathway involving oxidative addition of the aryl halide to (BINAP)Pd as the first step, a pathway initiated by addition of the amine to the catalyst is proposed and supported by kinetic modeling of sequential reaction experiments. A subtle dependence of the reaction mechanism on the relative concentrations of substrates is revealed in these studies. The dependence of the catalyst resting state on reaction conditions is also discussed. This work suggests that conclusions from kinetic studies may be meaningful only for the conditions under which they are carried out, calling into question the use of conventional kinetic methods in this system.

Introduction

Over the past few years, the Pd-catalyzed amination of aryl halides has become a widely used synthetic method because of developments that have helped to improve selectivity and functional group tolerance.[1] Several recent kinetic and mechanistic studies of this reaction have focused on understanding the nature of the intermediate species in the catalytic cycle and on rationalizing the effects of different ligands and additives on its efficiency.[2] While the mechanism of the amination of aryl halides appears to be complex in comparison with the Heck,[3] Stille,[4] and Suzuki[5] reactions, it has generally been assumed that a feature common to C−C and C−N bond formation is the initial oxidative addition of the aryl halide to a Pd^0 complex. In the case of amination, oxidative addition is thought to be followed by coordination of the amine, deprotonation with base, and reductive elimination to yield the aryl amine (eq 1).[1c,d] Alternatively, Hartwig has suggested that oxidative addition of the aryl halide could be followed by reaction with the base to yield a Pd-alkoxide intermediate when DPPF is used as the ligand. This species then reacts with the amine to provide the (amido)aryl palladium species that undergoes reductive elimination.[1a,b]

* Address correspondence to these authors.
[†] Massachusetts Institute of Technology.
[‡] University of Hull.

(1) (a) Hartwig, J. F. *Angew. Chem., Int. Ed.* **1998**, *37*, 2046. (b) Hartwig, J. F.; Kawatsura, M.; Hauck, S. I.; Shaughnessy, K. H.; Alcazar-Roman, L. M. *J. Org. Chem.* **1999**, *64*, 5575. (c) Yang, B. H.; Buchwald, S. L. *J. Organomet. Chem.* **1999**, *576*, 125. (d) Wolfe, J. P.; Buchwald, S. L. *J. Org. Chem.* **2000**, *65*, 1144. (e) Wolfe, J. P.; Tomori, H.; Sadighi, J. P.; Yin, J. J.; Buchwald, S. L. *J. Org. Chem.* **2000**, *65*, 1158. (f) Muci, A. R.; Buchwald, S. L. *Top. Curr. Chem.* **2002**, *219*, 131.

(2) a) Alcazar-Roman, L. M.; Hartwig, J. F.; Rheingold, A. L.; Liable-Sands, L. M.; Guzei, I. A. *J. Am. Chem. Soc.* **2000**, *122*, 4618. (b) Guari, Y.; van Strijdonck, G. P. F.; Boele, M. D. K.; Reek, J. N. H.; Kamer, P. C. J.; van Leeuwen, P. W. N. M. *Chem.—Eur. J.* **2001**, *7*, 475.

(3) For reviews, see: (a) Brase, S.; de Meijere, A. In *Metal-Catalyzed Cross-Coupling Reactions*; Diederich, F., Stang, P. J., Eds.; Wiley-VCH: Weinheim, Germany, 1998; pp 99−166. (b) Beletskaya, I. P.; Cheprakov, A. V. *Chem. Rev.* **2000**, *100*, 3009. For mechanistic studies, see: (c) Amatore, C.; Broeker, G.; Jutand, A.; Khalil, F. *J. Am. Chem. Soc.* **1997**, *119*, 5176. (d) Tschoerner, M.; Pregosin, P. S.; Albinati, A. *Organometallics* **1999**, *18*, 670. (e) Hii, K. K.; Claridge, T. D. W.; Brown, J. M.; Smith, A.; Deeth, R. J. *Helv. Chim. Acta* **2001**, *84*, 3043 and references therein.

(4) For reviews, see: (a) Farina, V.; Krishnamurthy, V.; Scott, W. J. *Org. React.* **1997**, *50*, 1. (b) Mitchell, T. N. In *Metal-Catalyzed Cross-Coupling Reactions*; Diederich, F., Stang, P. J., Eds.; Wiley-VCH: Weinheim, Germany, 1998; pp 167−202. For mechanistic studies, see: (c) Casado, A. L.; Espinet, P.; Gallego, A. M.; Martinez-Ilarduya, J. M. *Chem. Commun.* **2001**, 339. (d) Amatore, C.; Bucaille, A.; Fuxa, A.; Jutand, A.; Meyer, G.; Ntepe, A. N. *Chem.—Eur. J.* **2001**, *7*, 2134. (e) Albeniz, A. C.; Espinet, P.; Martin-Ruiz, B. *Chem.—Eur. J.* **2001**, *7*, 11. (f) Ricci, A.; Angelucci, F.; Bassetti, M.; Lo Sterzo, C. *J. Am. Chem. Soc.* **2002**, *124*, 1060−1071 and references therein.

(5) For reviews, see: (a) Suzuki, A. In *Metal-Catalyzed Cross-Coupling Reactions*; Diederich, F., Stang, P. J., Eds.; Wiley-VCH: Weinheim, Germany, 1998; pp 49−98. (b) Suzuki, A. *J. Organomet. Chem.* **1999**, *576*, 147. For mechanistic studies, see: (c) Aliprantis, A. O.; Canary, J. W. *J. Am. Chem. Soc.* **1994**, *116*, 6985. (d) Ridgway, B. H.; Woerpel, K. A. *J. Org. Chem.* **1998**, *63*, 458 and references therein.

10.1021/ja026885r CCC: $22.00

The present paper reports kinetic studies of the Pd/BINAP-catalyzed amination of bromobenzene (**1**) with primary (*n*-hexylamine, **2a**) and secondary (*N*-methylpiperazine, **2b**) amines performed with reactant concentrations typical of those used in carrying out synthetic operations. In-situ experimental studies

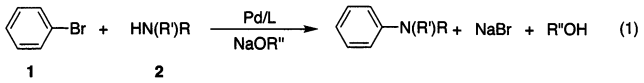

monitoring the entire course of the reaction were combined with a mechanistic approach to kinetic modeling to provide a detailed analysis of the reaction mechanism. The reaction exhibits an induction period which can mask the true kinetic dependences on substrate concentrations. A process for catalyst activation via binding of amine and loss of dba is proposed. Under conditions of excess amine, the reaction is well described by a simple kinetic model that involves amine binding to Pd prior to oxidative addition of the aryl halide. Our findings reveal that oxidative addition to (R(R′)NH)Pd(BINAP) proceeds faster than does oxidative addition to Pd(BINAP).

Background

The protocol used here for collecting and analyzing kinetic data differs from that of classical kinetic measurements and, for that reason, deserves some comment. Most kinetic studies of catalytic reactions are conducted under conditions far removed from those of practical synthesis. Concentration ratios are typically distorted in experiments designed to determine the individual concentration dependences of different reactants. In addition, initial rate measurements are often employed, typically when the catalyst has undergone only a very limited number of turnovers. Recent studies of Heck coupling reactions suggest, however, that results obtained in this way may provide a misleading mechanistic picture.[6,7] High excess concentration in one reactant can perturb the chemistry of the catalytic cycle, shifting the rate-limiting step and the relative abundance of different intermediates.[6] In addition, it has been shown that the slow activation of a precatalyst may be manifested as anomalous substrate concentration dependences.[7]

Scheme 1

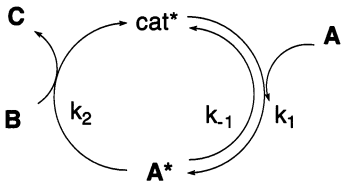

Consider as an example the two-substrate reaction shown in Scheme 1, involving the reversible binding of substrate **A** with a catalyst species cat* to form a reactive intermediate **A***, which adds substrate **B** to form the product **C** and complete the catalytic cycle. Application of steady-state kinetics gives the rate expression shown in eq 2. This expression is complex because it contains both substrate concentrations as variables. However, when [**A**] and [**B**], respectively, are held constant in high excess as in classical kinetic measurements, eq 2 reduces to the simple first-order kinetics shown in eqs 3 and 4. While this aids in determining the reaction orders in substrate concentrations, the separate determination of the individual elementary step rate constants is more difficult in such experiments.

$$r = \frac{k_1 k_2 [\mathbf{A}][\mathbf{B}][\mathrm{cat}]_{\mathrm{total}}}{k_{-1} + k_1[\mathbf{A}] + k_2[\mathbf{B}]} \tag{2}$$

$$r = \frac{-\mathrm{d}[\mathbf{B}]}{\mathrm{d}t} = k_{\mathrm{obs}}[\mathbf{B}] \quad [\mathbf{A}] \gg [\mathbf{B}];$$

$$k_{\mathrm{obs}} = \frac{k_1 k_2 [\mathbf{A}][\mathrm{cat}]_{\mathrm{total}}}{k_{-1} + k_2([\mathbf{B}]_0 - [\mathbf{A}]_0) + (k_1 + k_2)[\mathbf{A}]} \tag{3}$$

$$r = \frac{-\mathrm{d}[\mathbf{A}]}{\mathrm{d}t} = k'_{\mathrm{obs}}[\mathbf{A}] \quad [\mathbf{B}] \gg [\mathbf{A}];$$

$$k_{\mathrm{obs}} = \frac{k_1 k_2 [\mathbf{B}][\mathrm{cat}]_{\mathrm{total}}}{k_{-1} + k_1([\mathbf{A}]_0 - [\mathbf{B}]_0) + (k_1 + k_2)[\mathbf{B}]} \tag{4}$$

Before the advent of powerful computer methods and accurate in-situ experimental tools, extracting the concentration dependences in eq 2 was not possible without resorting to the simplifications of eqs 3 and 4. However, the combination of accurate and voluminous data collection together with computer simulations allows us to treat the full rate expression of eq 2 directly without mathematical simplification. Since there is no need to hold each concentration variable constant in turn, reactions may be carried out under conditions much closer to those employed in typical synthetic operations. In these concentration ranges, neither substrate is present in large excess, and both substrates [**A**] and [**B**] change simultaneously and continuously over the course of the reaction.

The protocol we outline here uses the in-situ experimental method of reaction calorimetry (see Experimental Section) to provide an accurate concentration profile over the course of a reaction carried out using synthetically relevant substrate concentration ratios. Each datum point during a reaction (typically collected every 2−30 s) is equivalent to a separate classical kinetic experiment at a different set of substrate concentrations. Thus, a single reaction can contain information equivalent to that which would require *hundreds* of separate classical kinetic measurements to obtain. These data are then compared to computer simulations of eq 2. Good agreement between the experimental data and the kinetic model helps to lend support to the mechanistic proposal; poor agreement suggests that the proposed mechanism may not be valid. In addition, the computer simulation provides a unique solution for the individual elementary step rate constants in the expression.[8] With these constants in hand, extrapolation of mechanistic conclusions to other experimental conditions is straightforward. For example, this may be used to help predict cases where the rate-limiting step shifts during the course of the reaction.[6]

It is important to note that the experimental protocol using continuously changing concentrations and eq 2 involves no loss of accuracy compared to those of experiments which make use of the simplified eqs 3 and 4. Similarly, it should be emphasized

(6) Rosner, T.; Le Bars, J.; Pfaltz, A.; Blackmond, D. G. *J. Am. Chem. Soc.* **2001**, *123*, 1848.
(7) Rosner, T.; Pfaltz, A.; Blackmond, D. G. *J. Am. Chem. Soc.* **2001**, *123*, 4621.
(8) The data required to obtain a unique solution may be determined for a particular mechanistic model. For example, in the catalytic cycle shown in Scheme 1, two experiments carried out at different initial concentrations of the two substrates such that the quantity $([A]_0 - [B]_0)$ is different for the two reactions were sufficient to provide a unique solution for the three elementary step rate constants.

that the use of eqs 3 and 4 simplifies only the mathematics, but not the chemistry, of the system under study.

The relative concentrations of catalytic species for the example in Scheme 1 can be derived from eq 2 and are shown in eqs 5 and 6. These equations demonstrate how the catalyst species partitioning between [cat*] and [**A***] within the cycle depends on substrate concentrations. Quantitative determination of the relative fractions of different species is only possible when the individual rate constants are known. Since these values are not obtained in classical kinetic experiments, it is often assumed that one species within the cycle may be identified as the "resting state" of the catalyst. For example, in the cycle shown in Scheme 1, the resting state of the catalyst under conditions where eq 3 holds may be the intermediate species [**A***] formed when [**A**] binds to the catalyst. Under conditions where eq 4 holds, the resting state may be the unligated catalyst species [cat*]. When neither substrate is present in large excess, however, it may happen that either no single dominant resting state exists or else the resting state will change over the course of the reaction. This will often be the case for reactions carried out under synthetically relevant conditions. Mechanistic insights based on the altered conditions of the classical measurement may thus provide a distorted view of the partitioning of the catalytic species in the reaction, as it will be carried out practically. This may occur even without taking into account the possibility that different mechanisms may operate at very different substrate concentrations.[9,10]

$$[\mathrm{cat}*] = \frac{k_{-1} + k_2[\mathbf{B}]}{k_{-1} + k_1[\mathbf{A}] + k_2[\mathbf{B}]}[\mathrm{cat}]_{\mathrm{total}} \quad (5)$$

$$[\mathbf{A}*] = \frac{k_1[\mathbf{A}]}{k_{-1} + k_1[\mathbf{A}] + k_2[\mathbf{B}]}[\mathrm{cat}]_{\mathrm{total}} \quad (6)$$

An important consideration in kinetic measurements either by classical methods using eqs 3 and 4 or in our protocol using eq 2 is that the total concentration of catalyst within the catalytic cycle $[\mathrm{cat}]_{\mathrm{total}}$ is assumed to be constant. If this is not the case, anomalous reaction orders in substrate may be observed.[7] A decrease in $[\mathrm{cat}]_{\mathrm{total}}$ due to catalyst deactivation will affect k_{obs} in eqs 3 and 4, and the reaction order in [**A**] and [**B**] will thus appear to be *higher* than the true kinetic order. Similarly, an increase in $[\mathrm{cat}]_{\mathrm{total}}$ during the reaction will cause the reaction orders in substrate to appear *lower* than their true kinetic order.

It may also be the case that some fraction of the catalyst is present in the form of inactive species not participating in the catalytic cycle, even for a system at steady state. Such spectator species may often be observable by spectroscopic methods, even when catalyst species active within the network are not. However, monitoring the reaction kinetics can help to provide clues about the species in the catalytic cycle, even when they are not detectable by other methods.

Experimental Section

General Considerations. Toluene was purchased from J. T. Baker in CYCLE-TAINER solvent delivery kegs and vigorously purged with argon for 2 h. The solvent was further purified by passing it under argon pressure through two packed columns of alumina and copper-(II) oxide.[11] Bromobenzene **1** was purchased from Lancaster and further purified by washing with concentrated H_2SO_4 and then washing with a saturated solution of $NaHCO_3$, followed by distillation from CaH_2. *N*-methylpiperazine (**2b**) and *n*-hexylamine (**2a**) were purchased from Aldrich Chemical Co. and distilled from CaH_2 prior to use. Tris-(dibenzylideneacetone)dipalladium(0) and (*S*)-BINAP were acquired from Strem Chemicals, Inc. and used without further purification. Sodium *tert*-amylate (NaO*t*Am) was purchased from Aldrich. All reagents were handled and stored in a nitrogen-filled glovebox. Chromatographic measurements were recorded on an Agilent 6890 Series GC system. ^{1}H NMR spectra were obtained on Bruker AM 400 MHz, Varian Mercury 300 MHz, or Varian Unity 300 MHz Fourier transform NMR spectrometers. ^{31}P{^{1}H} NMR spectra were obtained on a Varian Mercury 300 MHz spectrometer operating at the corresponding frequency.

Material Preparation. (*S*)-(BINAP)Pd(dba) was prepared as previously reported.[12] $Pd(BINAP)_2$ was prepared as follows.[13] A solution of NaOH (0.24 g, 6.0 mmol) in MeOH (5 mL) was added to a yellow heterogeneous mixture of $[Pd(allyl)Cl]_2$ (0.04 g, 0.11 mmol) in MeOH (3 mL). The resulting clear yellow solution was degassed by three freeze−pump−thaw cycles, and (*S*)-BINAP (0.27 g, 0.43 mmol) in toluene (10 mL) was added to give a dark red solution. After additional degassing (three times), the mixture was stirred overnight at room temperature. The solvent was removed in vacuo on a Schlenk line, washed with MeOH (2 × 5 mL), and dried under vacuum to afford a dark red solid (0.115 g, 0.09 mmol, 78%). ^{1}H NMR (400 MHz, C_6D_6): δ 8.37 (br s, 8H), 7.82 (br d, 4H), 7.45 (br s, 8H), 7.33−7.39 (m, 8H), 7.18−7.29 (m, 16H), 7.03−7.08 (m, 4H), 6.83−6.87 (m, 4H), 6.18 (t, J = 7.3 Hz, 4H), 5.88 (t, J = 7.6 Hz, 4H). ^{31}P NMR (C_6D_6): 27.8 (s).

Reaction Procedure. Reactions were performed in the Buchwald laboratories at MIT in a stirred 16-mL screw capped vial with a PTFE septa under a positive pressure of argon. The reaction vial (typically 4.2-mL reaction volume) was placed in the sample compartment of a reaction calorimeter (Omnical, SuperCRC) with an empty vial placed in the reference compartment. The stirred vial was maintained under isothermal conditions at 333 K. The calorimeter recorded the difference in heat flows from the sample versus reference cells at data collection rates up to 30 min^{-1} (2 min^{-1} used in this work). Reactions were initiated by adding one component to a thermally equilibrated reaction mixture containing all of the other components. Initial concentrations of different components were varied within synthetically useful ranges, as given in the Results Section. A typical reaction was conducted by adding $Pd_2(dba)_3$ and BINAP (Pd/L = 1:1; 2 mol % Pd based on the concentration of **1** unless otherwise noted) in toluene to a thermally equilibrated reaction mixture consisting of 0.71 M bromobenzene, 1.07 M *N*-methylpiperazine, 1.0 M NaO*t*Am, and dodecane as an internal standard. The reaction mixture was in each case a yellow homogeneous solution. The order of addition and mixing time of substrates and catalyst was also varied as described in the text.

Kinetic Data Analysis. The use of reaction calorimetry to study reaction kinetics has been described previously.[14] An energy balance around the reaction vessel demonstrates that, for the case of a single reaction occurring, the reaction heat flow, q, is proportional to the

(9) Alcazar-Roman, L. M.; Hartwig, J. F. *Organometallics* **2002**, *21*, 491.
(10) In ref 9, Hartwig and co-workers found that kinetic studies of the oxidative addition of **1** to $Pd(BINAP)_2$ carried out at [**1**] < 0.1 M were not in agreement with those carried out at substrate concentrations of 0.5−4 M. They invoked a change in mechanism to rationalize these results.

(11) (a) Pangborn, A. B.; Giardello, M. A.; Grubbs, R. H.; Rosen, R. K.; Timmers, F. J. *Organometallics* **1996,** *15*, 1518. (b) Alaimo, P. J.; Peters, D. W.; Arnold, J.; Bergman, R. G. *J. Chem. Educ.* **2001**, *78*, 64.
(12) Wolfe, J. P.; Wagaw, S.; Buchwald, S. L. *J. Am. Chem. Soc.* **1996**, *118*, 7215.
(13) Bolm, C.; Kaufmann, D.; Gessler, S.; Harms, K. *J. Organomet. Chem.* **1995**, *502*, 47−52.
(14) (a) Blackmond, D. G.; McMillan, C. R.; Ramdeehul, S.; Schorm, A.; Brown, J. *J. Am. Chem. Soc.* **2001**, *123*, 10103. (b) Rosner, T.; Sears, P. J.; Nugent, W. A.; Blackmond, D. G. *Org. Lett.* **2000**, *2*, 2511. (c) LeBlond, C.; Wang, J.; Larsen, R. D.; Orella, C. J.; Forman, A. L.; Landau, R. N.; Laquidara, J.; Sowa, J. R., Jr.; Blackmond, D. G.; Sun, Y.-K. *Thermochim. Acta* **1996**, *289*, 189.

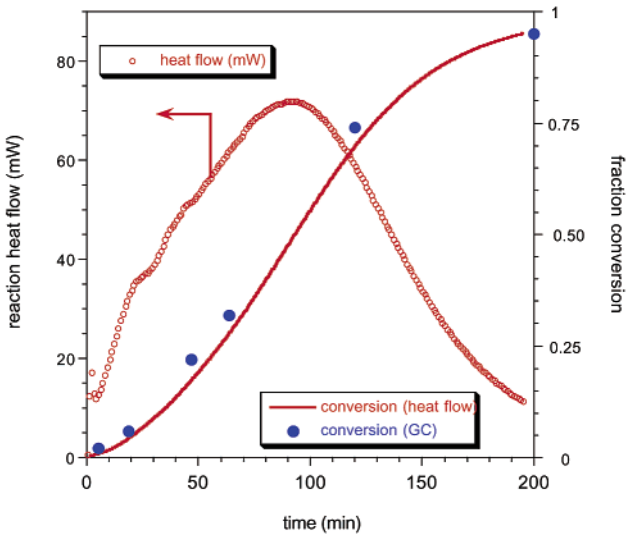

Figure 1. Reaction heat flow and fraction conversion vs time for the amination of bromobenzene (**1**, 0.71 M) with *N*-methylpiperazine (**2b**, 0.86 M) using NaO*t*Am (1.0 M) as base and a 0.5:1 mixture of $Pd_2(dba)_3$ and BINAP (2 mol % Pd based on $[\mathbf{1}]_0$) as catalyst.

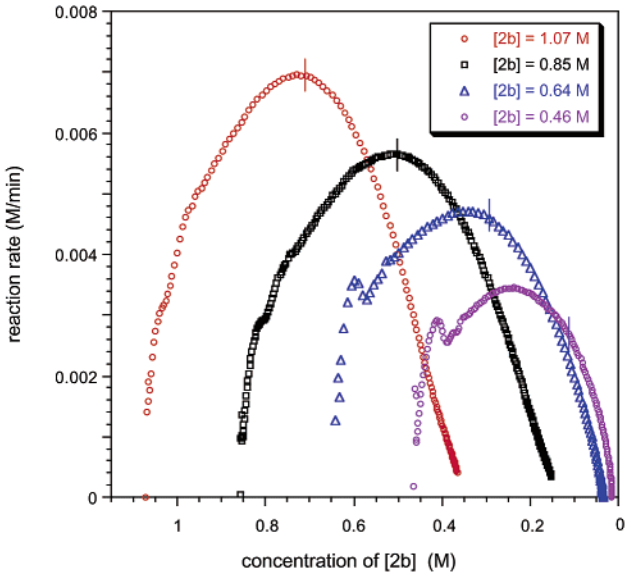

Figure 2. Reaction rate vs concentration [**2b**] for the amination of **1** with [**2b**]. $[\mathbf{1}]_0 = 0.71$ M; initial concentrations of $[\mathbf{2b}]_0$ as listed in the figure; $[NaOtAm]_0 = 1.0$ M (1.4 equivalents); 1:1 Pd/BINAP from $Pd_2(dba)_3$ 2 mol % Pd based on $[\mathbf{1}]_0$. Vertical lines mark [**1**] = 0.35 M during each reaction. Vertical hatch marks show the point where [**1**] = 0.35 M in each reaction.

reaction rate, r, where ΔH_{rxn} is the heat of reaction and V is the reaction volume.

$$q = \Delta H_{rxn} V r \tag{7}$$

The heat of reaction from integration of the observed heat flow versus time curves gave an average value of 182 kJ/mol ± 5%. The observed heat flow profiles can be used to obtain the fractional conversion of aryl halides by calculation of the fractional area under the temporal heat flow curve by eq 8, where the numerator represents the area under the heat flow to any time point t and the denominator represents the total area under the heat flow curve.

$$\text{fractional conversion} = \frac{\int_0^t q\,dt}{\int_0^{t_f} q\,dt} \tag{8}$$

Kinetic parameters were determined by fitting the reaction rate data obtained from the heat flow to an analytical rate equation using the Solver program in Excel (Microsoft).

Results

Figure 1 shows a typical reaction heat flow profile as a function of time for an amination reaction initiated by adding a mixture of $Pd_2(dba)_3$ and BINAP (2 mol % Pd based on **1**) in toluene to a reaction vial containing 0.71 M bromobenzene (**1**), 1.07 M *N*-methylpiperazine (**2b**), and 1.0 M NaO*t*Am at 60 °C. Conversions obtained both from the heat flow (eq 8, solid line in Figure 1) and from gas chromatographic analysis of side by side reactions (data points in Figure 1) are also shown in the figure. The excellent correlation between data obtained from these different methods confirms that the heat flow profile provides a valid measure of reaction rate in this case.

The heat flow curve in Figure 1 exhibits an unusual form, rising gradually for more than 1 h before attaining a maximum after more than 50% of the aryl bromide was consumed, equivalent to ~25 turnovers. This apparent negative order behavior in substrate concentration is in contrast with the cases of most catalytic reactions, which typically exhibit positive dependences on substrate concentrations or dependences that vary between zero and a positive order as substrate concentrations decrease.

Figure 2 shows the rate profile for reactions carried out by varying the initial concentration of *N*-methylpiperazine (**2b**), while employing the same initial concentration of the aryl bromide, base, and catalyst. Plotted here as reaction rate versus amine concentration [**2b**], in all cases the reaction showed a characteristic rise in rate over the first half of the reaction before assuming positive order kinetics in substrates. The positive dependence on [**1**] may be seen by examining the rates of different reactions as they intersect any vertical line drawn in Figure 2, which represents equal concentrations of **2b** and different concentrations of **1** for the different reactions. The positive order in [**2b**] may also be discerned by identifying sets of data points corresponding to different concentrations of **2b** at equal concentrations of **1**; one such set of points is highlighted in Figure 2 by the small vertical lines marking the point where [**1**] = 0.35 M in each of the four reactions. Reactions with the primary amine **2a** also exhibited an induction period, although it was less significant, with the rate reaching a maximum at ~20% conversion, or 10 turnovers.

The induction behavior was unaffected by changes in a number of reaction variables. Virtually superimposable rate curves were obtained with base concentrations of 1.4 and 2 equiv compared to that of the aryl bromide, as shown in Figure 3. If the base was present in substoichiometric amounts, however, the rate became suppressed at higher conversions. Figure 3 also shows that the addition of 17 equiv of NaBr compared to Pd did not influence the induction period and gave a maximum rate within 10% of the reaction without added NaBr. The use of a preformed (dba)Pd(BINAP) complex as the precatalyst resulted in rate curves with induction periods similar to those observed with reactions using $Pd_2(dba)_3$/BINAP mixtures, although the maximum rate was ~20% higher for reactions using this complex (Figure 3).

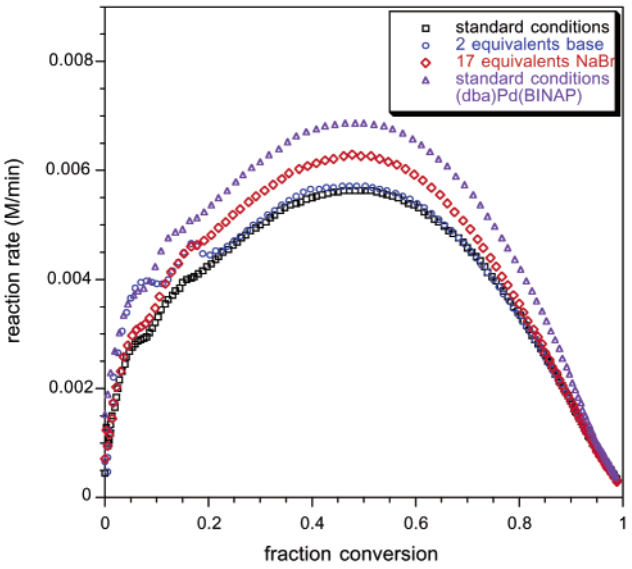

Figure 3. Reaction rate vs fraction conversion for the amination of [**1**] with [**2b**]. (○) Standard conditions defined as initial concentrations $[\mathbf{1}]_0 =$ 0.71 M; $[\mathbf{2b}]_0 = 0.86$ M; $[\text{NaO}t\text{Am}]_0 = 1.0$ M; 1:1 Pd/BINAP from $Pd_2(dba)_3$ 2 mol % Pd based on $[\mathbf{1}]_0$. (□) Standard conditions except 1.5 M base (2 equiv). (◇) Standard conditions except 17 equiv of NaBr added to the reaction mixture. (△) Standard conditions except (dba)Pd(BINAP) used as catalyst.

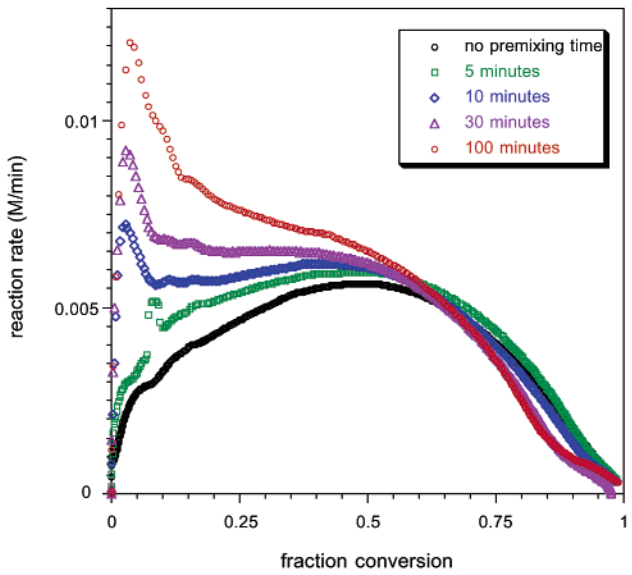

Figure 4. Reaction rate vs fraction conversion of [**1**] as a function of the premixing time of all components prior to the addition of **1** to the reaction mixture. Bromobenzene (**1**, 0.71 M) with *N*-methylpiperazine (**2b**, 0.86 M) using NaO*t*Am (1.0 M) as base and a 0.5:1 mixture of $Pd_2(dba)_3$ and BINAP (2 mol % Pd based on $[1]_0$) as catalyst. Time of premixing as given in the figure.

Reactions were also carried out using the isolated complex (BINAP)Pd(*p*-tolyl)Br as the precatalyst. This reaction was extremely rapid, requiring less than 1 min to complete one turnover of [**1**], at which time all of the precursor (BINAP)-Pd(*p*-tolyl)Br has presumably been consumed. However, the reaction still exhibited an induction period similar to that observed using $Pd_2(dba)_3$/BINAP mixtures and the isolated Pd-(dba)(BINAP). At its maximum (which occurred after ~20 turnovers), the rate was 15 times greater than the peak rate for $Pd_2(dba)_3$/BINAP. However, the reaction rate rapidly declined after this maximum, suggesting deactivation of the active catalyst species.

The induction period was influenced by the order in which reagents were mixed and by the mixing time between components prior to initiation of the reaction. Figure 4 shows the effect of varying the time of premixing $Pd_2(dba)_3$ and BINAP with the base and amine in the reaction vial. Increased amine-catalyst interaction resulted in positive order initial rate profiles and significantly higher initial rates than those in reactions where the catalyst was added last. The high initial rate eventually gave way to the characteristic rate profile observed in Figure 2 for reactions carried out without catalyst premixing. This behavior is suggestive of the combination of multiple reaction pathways.

An experimental protocol involving a series of sequential reactions in a single vessel was designed both to provide further insight into the induction period and to aid in kinetic modeling. The reaction is initiated by adding an aliquot of substrate **1** to a reaction mixture containing all other reagents. Concentrations of the amine **2a** or **2b** and the base are in sufficient excess to allow full conversion of multiple sequential aliquots of **1**, each reaction initiated by injection of a further aliquot of **1** in the same vessel. The number of turnovers previously experienced by the catalyst increases with each aliquot of **1** reacted. Therefore, we may infer that a steady state in catalyst concentration has been attained by observation of sequential injections exhibiting well-behaved kinetic profiles. Moreover, each injection corresponds to a different ratio of substrate concentrations [**1**]:[**2**]. Comparing the rate profiles of well-behaved reactions employing different relative concentrations provides sufficient data for kinetic modeling. On the basis of the results from the modeling, information regarding the concentration dependences in both substrates can be obtained, which ultimately leads to the development of the reaction rate law.

Figure 5a and b show two sets of these reactions carried out with sequential injections of four aliquots of **1** into a mixture containing Pd_2dba_3 and BINAP, NaO*t*Am, and either **2a** (*n*-hexylamine) or **2b** (*N*-methylpiperazine). The Pd concentration is ~11 mol % on the basis of each aliquot of **1**, corresponding to 2.7 mol % Pd based on the total four-reaction sequence. Figure 5b shows that, for **2b**, the first injection in the sequence exhibited a lower initial rate and rate profile similar to those observed in the reactions shown in Figure 4 with long premixing times for the amine and catalyst. The three following reactions exhibited high initial rates, no induction period, and well-behaved positive order rate profiles. Figure 5a shows that, for **2a**, all reactions in the series gave positive order rate profiles, and the rate of the first reaction was only slightly lower than that of the second. The positive slope of each rate profile and the progressively lower peak heights for these sequential reactions suggest a positive rate dependence on both amine and bromobenzene concentrations.

When this injection protocol was carried out using $Pd(BINAP)_2$ as the precatalyst, the results obtained were significantly different, as shown in Figure 6 for reactions of **1** with **2b**. The initial injection showed transient behavior similar to that observed in the initial injection for this reaction using $Pd_2(dba)_3$ and BINAP. However, for each subsequent injection in the series using $Pd(BINAP)_2$, the initial reaction rate was *higher* rather than lower. The concave shape of the rate curves became less pronounced with each injection, as is demonstrated

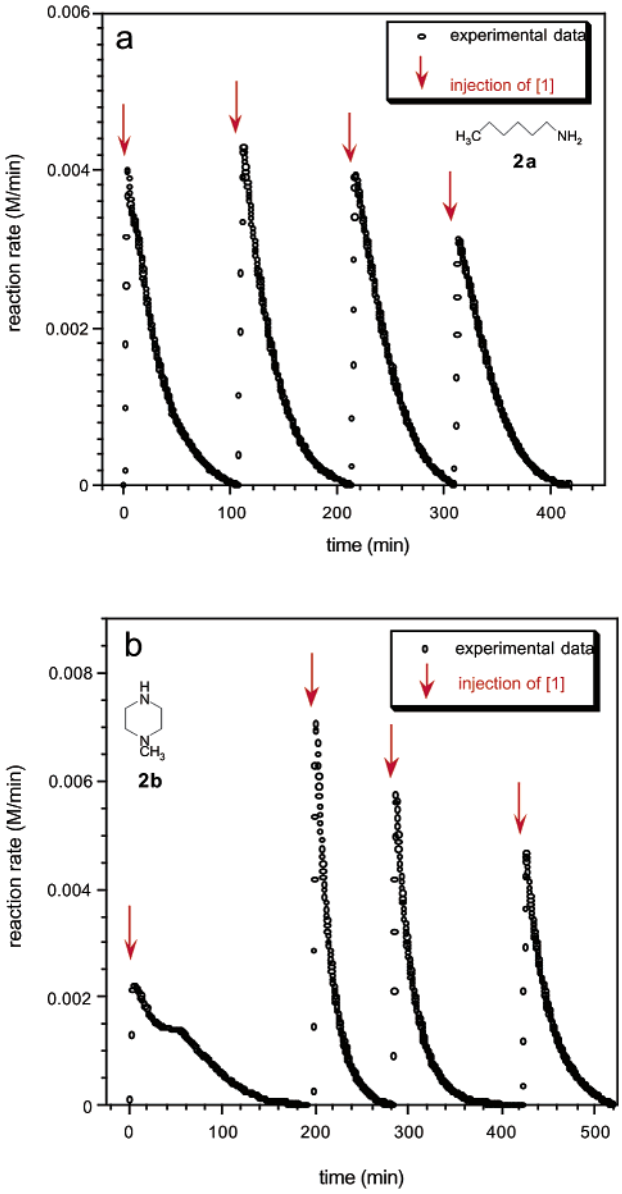

Figure 5. Consecutive reactions with added aliquots of PhBr ([**1**] = 0.13 M) with (a) *n*-hexylamine ([**2a**]$_0$ = 0.86 M)) and (b) *N*-methylpiperazine ([**2b**]$_0$ = 0.86 M), using NaO*t*Am (1 M) as base and a 0.5:1 mixture of $Pd_2(dba)_3$ and BINAP (11 mol % based on each aliquot of [**1**]$_0$). Points of injection of **1** are marked with ↓.

in Figure 7b, where the reaction rate is plotted versus concentration of **1** for the second, third, and fourth injections. With each consecutive reaction, the slope of the rate curve becomes more positive and shows less curvature, indicating an increase in the overall observed reaction order with each progressive reaction from close to zero order toward first order. When this series of reactions was carried out with excess BINAP added to the reaction mixture, similar behavior was observed. Although in this case, the overall rate was significantly suppressed, decreasing by a factor of 3 when 0.3 equiv of excess BINAP was added. When 1 equiv of excess BINAP was added, the rate became too slow to measure by reaction calorimetry.

Attempts to carry out this sequential injection protocol in reverse (injecting sequential aliquots of the amine into a reaction solution containing the catalyst, aryl bromide, and the base) were unsuccessful for either precatalyst. With a large excess of aryl

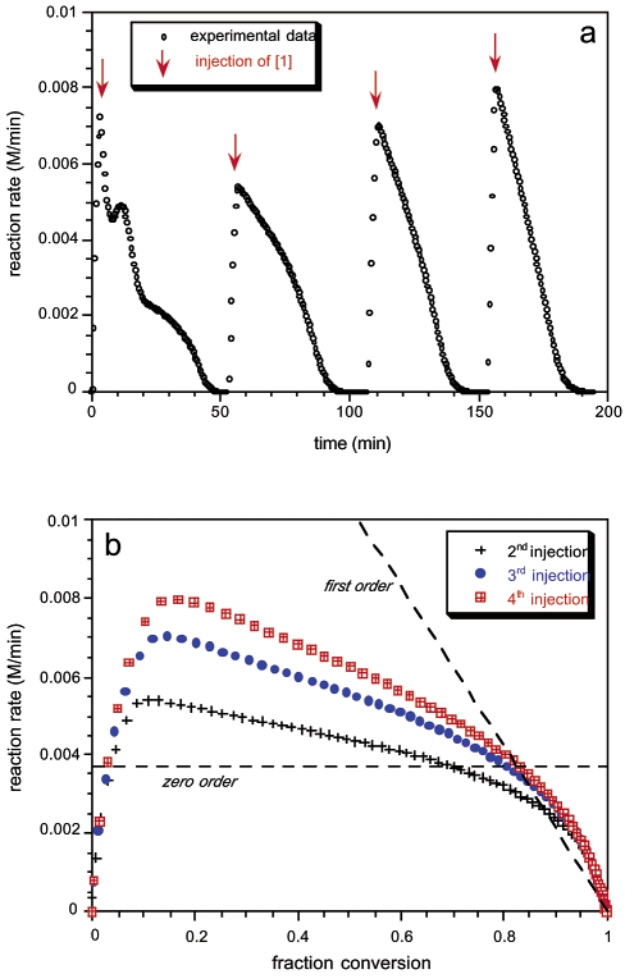

Figure 6. (a) Consecutive reactions with added aliquots of PhBr ([**1**] = 0.13 M) with *N*-methylpiperazine ([**2b**]$_0$ = 0.86 M) using NaO*t*-Am (1 M) as base and $Pd(BINAP)_2$ (9.1 mol % based on each aliquot of [**1**]$_0$). Points of injection of **1** are marked with ↓. (b) Injections 2, 3, and 4 are plotted as rate vs fraction conversion.

bromide, either the catalyst deactivated or the reaction proceeded too slowly to monitor by reaction calorimetry.

Discussion

Nature of the Induction Period. The curves in Figures 1−3 for reactions where $Pd_2(dba)_3$/BINAP mixtures and the (dba)-Pd(BINAP) complex were used as precatalysts are consistent with Amatore's detailed studies describing the slow dissociation of dba from Pd complexes.[15] In addition, the shape of the curves closely resemble those of rate curves that have been reported for Heck coupling reactions using slowly dissociating palladacycles as catalyst precursors.[7] This suggests that the behavior observed here is due to the slow reaction of the precatalyst, resulting in a gradual increase in the amount of active Pd catalyst present in the catalytic cycle. Amatore has shown that oxidative addition to the three-coordinate (dba)Pd(BINAP) can occur without the dissociation of dba, although Pd(BINAP) is more active.[14b] We suggest that the increasing rate is due to an increasing concentration of Pd(BINAP) formed from dissociation of the dba from (dba)Pd(BINAP), since similar catalytic

(15) (a) Amatore, C.; Jutand, A.; Khalil, F.; M′Barki, M. A.; Mottier, L. *Organometallics* **1993**, *12*, 3168. (b) Amatore, C.; Broeker, G.; Jutand, A.; Khalil, F. *J. Am. Chem. Soc.* **1997**, *119*, 5176. (c) Amatore, C.; Jutand, A. *Coord. Chem. Rev.* **1998**, *178*−*180*, 511.

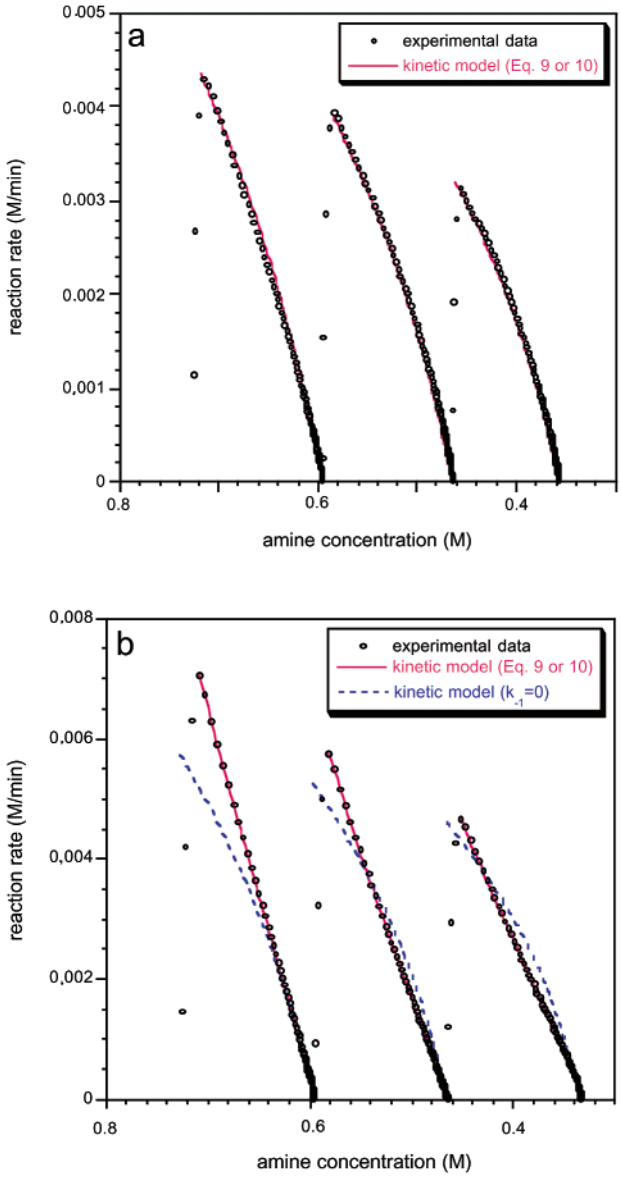

Figure 7. Comparison of experimental data to the kinetic model as based on eqs 9 and 10, plotted as reaction rate vs amine concentration. Points of injection of **1** are marked with ↓. Data are from reactions shown in Figure 5 of $Pd_2(dba)_3$/BINAP and **1** with (a) primary amine **2a** and (b) secondary amine **2b**.

behavior was observed when we used either preformed (dba)-Pd(BINAP) complex or $Pd_2(dba)_3$/BINAP mixtures. Under reaction conditions, this is considered to be virtually irreversible because of the low concentration of dba and the probability that it is destroyed through a subsequent reaction with amine or base.[16]

Although the presence of an induction period in this catalyst system could be predicted from Amatore's stoichiometric studies of the Pd(dba)/(BINAP) system[15b] and other complexes,[15a] the current work reveals the significant extent to which the overall catalytic behavior may be influenced. This work also highlights in general how such rate behavior may complicate attempts to determine kinetic rate laws for the catalytic reaction. Figure 2 confirms that the reaction rate exhibits a positive-order dependence on both bromobenzene and amine concentrations, but it also shows that the intrinsic kinetic dependences are convoluted by the changing concentration of active Pd. In such cases, the reliable determination of reaction orders cannot be made by simple initial rate or single-point rate measurements.

In two recent kinetic studies on the amination reaction using different Pd precatalysts, anomalous zero-order dependences on substrates were reported. Using Pd^0(bisphosphine) complexes, van Leeuwen and co-workers[2b] observed an induction period when the reactions were carried out in the absence of added halide ions, along with a zero-order dependence on aryl halide and amine and a nonfirst-order dependence on [Pd]. Hartwig and co-workers also reported zero-order substrate dependences using $Pd(BINAP)_2$ complexes as catalysts. The kinetic considerations discussed above combined with recent findings[7] present an alternate rationalization of these observations. As described in the Background section of this paper and in ref 7, an observation of *apparent* zero-order kinetics in substrates may be made if the observed rate is limited by an external step which increases the concentration of active Pd within the cycle.

The consecutive reaction protocol shown in Figure 6 for Pd-$(BINAP)_2$ precatalysts helps to illustrate this point. Hartwig and co-workers[2a] attributed their observation of zero-order kinetics in substrate for reactions employing primary amines to a mechanism in which $Pd(BINAP)_2$ lies directly on the catalytic cycle. The same mechanism was also invoked for reactions with secondary amines, with observed deviations from zero-order behavior attributed to catalyst deactivation or product inhibition. If this mechanism holds, a plot of rate versus time should be a straight line with zero slope for primary amines, and consecutive reactions should give identical plots. For secondary amines, deactivation or inhibition of the active catalyst should be reflected in decreasing peak heights for each consecutive reaction. However, the rate curves for the reactions in Figure 6 did not show this behavior. The *increase* in rate observed with each subsequent reaction of aliquots of **1** using $Pd(BINAP)_2$ is consistent with neither a constant nor decreasing concentration of $Pd(BINAP)_2$ within the cycle. These results suggest instead that the concentration of the active Pd(BINAP) catalyst within the cycle is *increasing* over time because of the slow loss of a BINAP ligand from $Pd(BINAP)_2$ lying *external* to the cycle. The shift in the observed overall reaction order from close to zero-order toward first-order kinetics shown in Figure 6b is also consistent with this proposal, as discussed in the Background section. As a larger fraction of the Pd is introduced into the catalytic cycle, the observed kinetics begin to manifest the true positive reaction orders in substrate.

It should be noted that the reactions reported by Hartwig and co-workers[2a] were carried out using 10 mol % $Pd(BINAP)_2$, which corresponds approximately to the same number of turnovers completed in the first injection shown in Figure 6, at which point the catalyst concentration had clearly not attained a steady state. Indeed, under our conditions, the data shown in Figure 7b suggest that the catalyst was not completely activated even after 40 turnovers, the equivalent of a reaction carried out at 2.5 mol % catalyst.

Reactions carried out using the preformed oxidative addition complex [(*p*-tolyl)Br]Pd(BINAP) as a precatalyst showed that such a species cannot be the predominant intermediate in the catalytic cycle. These reactions also exhibited an induction

(16) We are grateful to a referee for the suggestion concerning the interaction of base with dba.

Scheme 2. Mechanism for Activation of Pd(BINAP) from $Pd_2(dba)_3$/BINAP Mixtures[a]

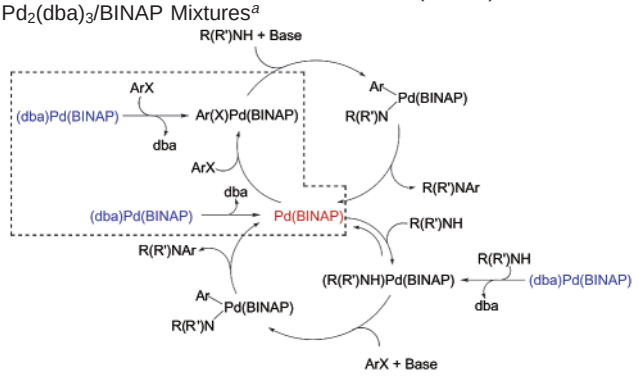

[a] The proposed reactions contained within the dashed lines are based on Amatore's studies[15b] of the oxidative addition of aryl halides to $Pd(dba)_2$/BINAP.

period, even after the rapid conversion of the precursor species. In addition, the maximum rate on a per Pd basis was significantly higher than that observed using $Pd_2(dba)_3$/BINAP mixtures. The reaction using preformed (dba)Pd(BINAP) complex also gave a slightly higher maximum rate than that of $Pd_2(dba)_3$/BINAP mixtures. This suggests that the ultimate steady-state catalyst concentration of active Pd within the cycle is sensitive to the nature of the precursor. Even when a steady state is attained for catalysts using $Pd_2(dba)_3$ as a precursor, a significant portion of the total [Pd] may remain outside the catalytic cycle as an unreactive spectator species.

Proposed Mechanisms. Further mechanistic information is offered in the experiments varying the mixing time between the catalyst and the amine. The curves in Figure 4 suggest that a combination of fast and slow processes ultimately brings the catalyst to its steady-state concentration. Amatore and coworkers' detailed kinetic studies of the stoichiometric oxidative addition of ArI to (dba)Pd(BINAP) showed that addition to the complex without dba was much faster than addition to the complex with the dba ligand.[15b] The routes they proposed are represented by the pathways inside the dashed lines in Scheme 2, with the exception that we have depicted the elimination of dba as irreversible under our reaction conditions. Since, in our case, the fast initial reaction is related to the mixing time between the catalyst and the amine, we also propose two additional routes involving amine coordination, also shown in Scheme 2. The three-coordinate metal center (R(R′)NH)Pd(BINAP) produced upon substitution of amine for dba is more electron rich than (dba)Pd(BINAP) and could help accelerate the subsequent oxidative addition of the aryl bromide.[17] The amine association could be facilitated by the dissociation of one of the diphenylphosphino groups of BINAP, resulting in a two-coordinate Pd species.[18] The amine bound (monophosphine)Pd would also accelerate the oxidative addition process, since the metal center is more electron rich relative to a two-coordinate Pd(BINAP) species. Completion of the first turnover generates Pd(BINAP) or a solvated form of this complex, which from this point on serves as the entry point for the catalytic cycle. The fact that the induction period was less profound in the reaction of the primary amine **2a** is consistent with this proposal, since **2a** presents less steric hindrance to binding than does the secondary amine **2b**.[19]

Although the stoichiometric reaction in which the amine aids in the removal of dba would proceed for only the first turnover, this suggests that a viable catalytic cycle may also be proposed in which amine binding precedes oxidative addition of the aryl halide. Competition between the amine and the aryl bromide for the newly formed Pd(BINAP) catalyst may permit two separate viable catalytic cycles, depicted in Scheme 2. The degree to which each contributes to the overall rate may depend on the relative concentrations of amine and aryl bromide and their relative affinities for the catalyst. For the reactions in Figure 4, longer premixing times may help activate a larger fraction of the active catalyst via amine binding and dba elimination prior to introduction of [**1**]. The appearance of two separate rate processes, however, suggests that, after this first turnover, a significant fraction of the catalyst is diverted toward the pathway involving oxidative addition of [**1**] as the first step.

Kinetic Modeling of the Steady-State Catalytic Cycle. The quantitative determination of concentration dependences in aryl bromide and amine may be made using the consecutive reaction data shown in Figure 5a and b. The well-behaved reaction rate profiles observed after the first injection indicate that the active catalyst in the cycle has attained a constant concentration. The rate profiles for each individual reaction suggest positive order kinetics in bromobenzene, since the rate profiles decay as the concentration of bromobenzene decreases. Comparison of maximum peak heights for consecutive injections also suggest a positive dependence on amine concentration, since the initial amine concentration in the mixture was lower for each consecutive injection. Both of these observations are in agreement with the trends in Figure 2. The observation of identical rates for reactions using different base concentrations is consistent with a mechanism in which the base enters the catalytic cycle after the rate-limiting step. The suppression of the reaction rate at higher conversions when base was used as the limiting reagent suggests a shift in the rate-limiting step.

The simplest interpretation of these experimental results for trends in rate as a function of amine, aryl halide, and base concentrations suggests two possible mechanisms, shown in Schemes 3 and 4, which represent in more detail the two catalytic cycles depicted in Scheme 2. Scheme 3 depicts the conventional pathway, where oxidative addition of the aryl bromide occurs first, and Scheme 4 shows initial binding of the amine. For generality, the first step is shown as being reversible in both cases, although k_{-1} for the reductive elimination of PhBr shown in Scheme 2 is usually considered to be very small.[20]

Steady-state treatment of the reactive intermediates leads to the rate expressions shown in eqs 9 and 10 corresponding to the mechanisms shown in Schemes 3 and 4, respectively. Rate constants are defined in the schemes for the kinetically

(17) Collman, J. P.; Hegedus, L. S.; Norton, J. R.; Finke, R. G. *Principles and Applications of Organotransition Metal Chemistry*; University Science Books: Sausalito, CA, 1987; p 324.
(18) The dissociation of one of the diphenylphoshino groups of BINAP from $Pd(BINAP)_2$ to form a three-coordinate Pd species that undergoes oxidative addition has previously been suggested (refs 2a and 9).
(19) The addition of 60 equiv of **2a** to a 0.015 M solution containing (BINAP)Pd(dba) in d_8-toluene resulted in two new signals along with the signals corresponding to (BINAP)Pd(dba) in ^{31}P NMR. Upon heating at 60 °C for 90 min, the signal intensity of the two new peaks increased, while the ^{31}P signals for (BINAP)Pd(dba) decreased in intensity. Although the identity of the species corresponding to the new peaks in the ^{31}P NMR could not be determined unambiguously, this result indicates that the amine interacts with the precatalyst.
(20) Roy, A. H.; Hartwig, J. F. *J. Am. Chem. Soc.* **2001**, *123*, 1232.

Scheme 3

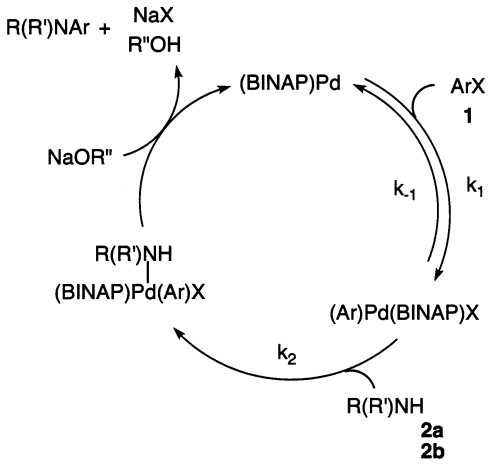

Scheme 4

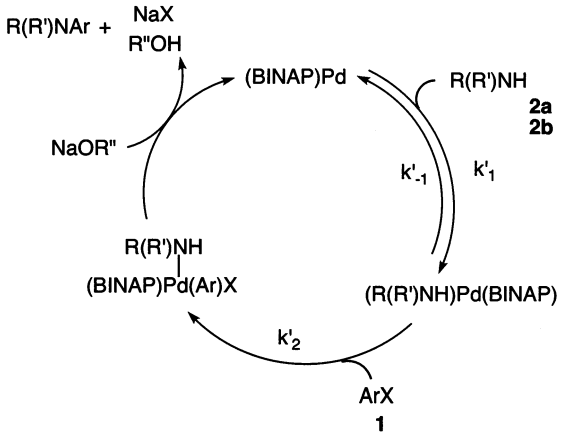

meaningful steps occurring prior to deprotonation with the base. $[Pd]_{total}$ refers to the total concentration of Pd added to the reaction.

$$\text{Scheme 3: (ArX first)} \quad \frac{k_1 k_2[\text{ArX}][\text{amine}][\text{Pd}]_{total}}{k_{-1} + k_1[\text{ArX}] + k_2[\text{amine}]} \tag{9}$$

$$\text{Scheme 4: (amine first)} \quad \frac{k_1' k_2[\text{ArX}][\text{amine}][\text{Pd}]_{total}}{k_{-1}' + k_1[\text{amine}] + k_1[\text{ArX}]} \tag{10}$$

Consideration of these equations reveals that the two mechanisms give mathematically equivalent reaction rate expressions, and only the physical meaning assigned to the rate constants differs from Scheme 3 to Scheme 4. Reaction simulations to this general form of the rate expression yield values for the rate constants which then may be examined to help choose which mechanism appears to be more consistent with general knowledge about the reaction system.

Figure 7 compares reaction simulations to the experimental data from Figure 5 for three consecutive reactions of both secondary and primary amines. The agreement between the experimental data and the simulation is excellent. The goodness of the fit to one simple equation for several sequential rate profiles over a range of relative substrate concentrations suggests that a single mechanism may dominate these reactions. Table 1 gives the rate constants predicted by the fit to the experimental data for each mechanism. Consideration of the relative magnitudes of these parameters helps to assess which mechanism gives a more realistic description of the observed reaction.

Table 1. Rate Constants Calculated from Reaction Simulations Optimized According to the Data in Figure 5a and b to Eqs 9 and 10[a]

	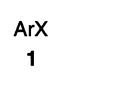 primary amine		 secondary amine	
model parameter	Eq. (9) Scheme 3	Eq. (10) Scheme 4	Eq. (9) Scheme 3	Eq. (10) Scheme 4
k_1 ($min.M^{-1}$)	4.43	1.06	37.00	2.88
k_{-1}(min^{-1})	0.05	0.05	11.88	11.88
k_2 ($min.M^{-1}$)	1.06	4.43	2.88	37.00
(k_1/k_{-1}) (M^{-1})	85.96	20.62	3.11	0.24

[a] Comparisons between experimental and simulated data are shown in Figure 7a and b.[21,22]

If Scheme 3 and eq 9 are valid, it is reasonable to assume that the rate constants for the oxidative addition of the aryl halide and its reductive elimination should be the same, regardless of whether a primary or secondary amine binds in the subsequent step. However, as shown in Table 1, these values differ significantly and predict dramatically different values of (k_1/k_{-1}) for the oxidative addition of [**1**] in the two cases. The model predicts an anomalously high rate of reductive elimination compared with the rate oxidative addition, especially for secondary amines. Indeed, the first step in Scheme 3 is most often written as irreversible; while fixing $k_{-1} = 0$ can provide a reasonably good fit of the data to the kinetic model for primary amines, such simulations resulted in an extremely poor fit to the experimental data for secondary amines, as shown in Figure 7b. Roy and Hartwig[20] have shown that the equilibrium constant for the oxidative addition/reductive elimination of aryl halides is very large ($K_{eq} = 10^2-10^5$), which is not consistent with the values of $k_1/k_{-1} = 3-85$ M^{-1} found here. Thus, we may conclude that Scheme 3 appears unlikely to be an accurate description of the reactions shown in Figure 5. Scheme 4, with amine binding preceding the oxidative addition of [**1**], provides a better description of the reaction under the conditions of these experiments, where [amine]/[PhBr] at the beginning of the reactions ranges from 5.6 to 3.6:1.

The parameters determined in the kinetic model for Scheme 4 provide further insight into the reaction mechanism. The model predicts that primary amines bind more strongly to the catalyst than do secondary amines. The stronger binding of primary amines may accelerate the catalyst activation process, consistent with the observation that the induction period is less significant for primary amines. This is in agreement with results of Amatore[15,17] concerning both electronic and steric effects on oxidative addition to Pd complexes.

The kinetic model also addresses the "resting state" of the catalyst species present within the catalytic cycle. The relative abundance of the catalytic intermediates within the cycle may be calculated according to eqs 11 and 12 under conditions where Scheme 4 holds. The relative fraction of species is dictated by both the concentration and the binding strength of the amine. Figure 8 illustrates how the resting state of the catalyst is a dynamic function of the concentrations of reactants and may change over the course of the reaction. For the primary amine (Figure 8a), the resting state of the catalyst is evenly divided between the two species at the beginning of the reaction, with

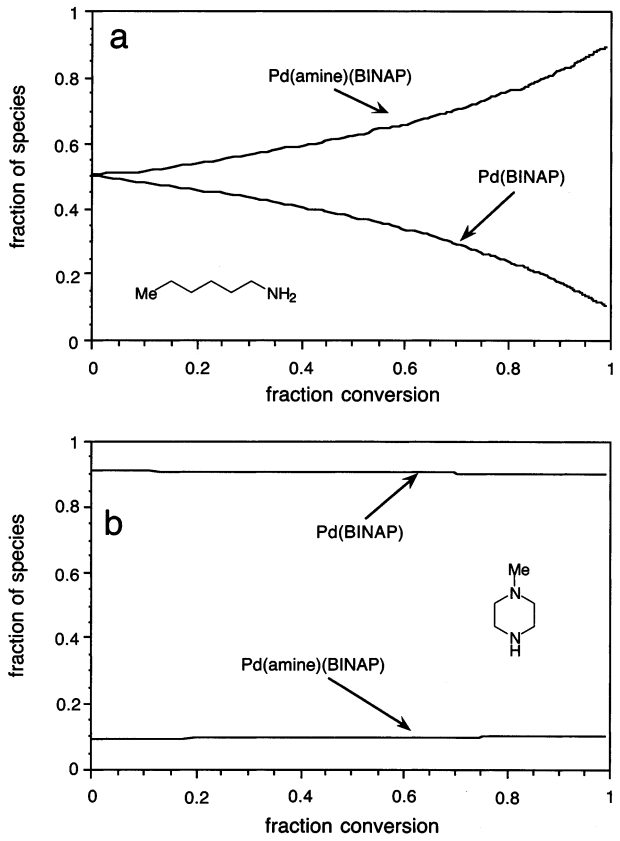

Figure 8. Relative fractions of the catalytic species Pd(BINAP) and (R(R′)-NH)Pd(BINAP) in Scheme 4 over the course of the reaction calculated using kinetic parameters taken from Table 1, according to eqs 11 and 12. Conditions correspond to the third injection in Figure 5, with $[\mathbf{1}]_0 = 0.13$ M and (a) $[\mathbf{2a}]_0 = 0.6$ M and (b) $[\mathbf{2b}]_0 = 0.6$ M.

(R(R′)NH)Pd(BINAP) increasing steadily over the course of the reaction. For the secondary amine, however, the unbound catalyst Pd(BINAP) remains ~90% of the Pd present within the catalytic cycle throughout the reaction (Figure 8b).

$$\frac{(\mathrm{R(R')NH)Pd(BINAP)}}{[\mathrm{Pd}]_{\mathrm{total}}} = \frac{k'_1[\mathrm{amine}]}{k'_{-1} + k'_{-1}[\mathrm{amine}] + k'_2[\mathrm{ArX}]} \tag{11}$$

$$\frac{\mathrm{Pd(BINAP)}}{[\mathrm{Pd}]_{\mathrm{total}}} = \frac{k'_{-1} + k'_2[\mathrm{ArX}]}{k'_{-1} + k'_1[\mathrm{amine}] + k'_2[\mathrm{ArX}]} \tag{12}$$

Figure 8 offers insight into the relative reactivity of Pd-(BINAP) and (R(R′)NH)Pd(BINAP) toward the oxidative addition of the aryl halide. Under conditions where a large fraction of the Pd within the cycle is present as Pd(BINAP), such as during the sequential reactions of **2b**, it might be reasonable to suppose that the aryl halide could compete successfully with the amine for Pd(BINAP). However, the results of the kinetic modeling demonstrate that oxidative addition to Pd(BINAP) (Scheme 3 pathway) made no significant contribution to the overall observed reaction which proceeded by the pathway in Scheme 4. This may be rationalized by comparing our reactions using $Pd(BINAP)_2$ with quantitative studies of the oxidative addition of **1** to $Pd(BINAP)_2$ by Hartwig and co-workers,[2a] allowing us to estimate that our reaction proceeded approximately 25 times faster than the oxidative addition of **1** to $Pd(BINAP)_2$ under similar conditions.[23] This suggests that the amine-binding route shown in Scheme 4 is significantly more efficient than reaction via the direct oxidative addition of the aryl halide to the Pd catalyst.

The calculation of the concentrations of catalyst intermediates, as shown in Figure 8, also demonstrates how the conditions of classical kinetic experiments, which generally employ a 10-fold difference in substrate concentrations, will present a distorted view of the resting state of the catalyst. For example, in reactions following Scheme 4 in which a 10-fold excess of ArBr is employed, the intermediate (R(R′)NH)Pd(BINAP) will account for less than 3% of the total *active* Pd for either secondary or primary amines.

It is important to emphasize that the active Pd species within the catalytic cycle may represent only a small fraction of the total Pd present. Indeed, results using different catalyst precursors suggest that, for the $Pd_2(dba)_3$/BINAP system, a significant concentration of Pd resides outside the catalytic cycle. Thus, a kinetic determination of catalytic intermediate species and resting state as described here provides a more meaningful mechanistic analysis relative to spectroscopic observations, which cannot distinguish between spectator and active species.

While the amine-binding cycle of Scheme 4 appears to dominate when the amine/bromobenzene ratio is high, the mechanism shown in Scheme 3 may become competitive under conditions of high [ArBr], complicating the determination of reaction orders and the distribution of catalyst intermediates. This may become an important concern in synthetic applications, typically carried out using a slight excess of amine. As the reaction progresses, the [amine]/[ArBr] ratio increases continuously as the limiting aryl bromide is consumed. Hence, it is likely that, under synthetically relevant conditions, the relative contribution to the overall rate from each of the pathways shown in Schemes 3 and 4 will change, even over the course of a single reaction. Such a subtle influence of substrate concentrations, which may not only alter the distribution of catalyst species but also change the reaction mechanism itself, emphasizes that in some cases the conclusions of a kinetic study may not be general but, instead, may apply quite narrowly to the specific conditions under which is it carried out.

Conclusions

Detailed kinetic studies of the amination of bromobenzene with primary and secondary amines using $Pd_2(dba)_3$/BINAP mixtures and $Pd(BINAP)_2$ provide significant mechanistic information and highlight the complexity of these reactions. The true kinetic dependences on substrate concentrations can be masked when there is a slow formation of the active catalyst that results in an induction period. The reaction is positive order in both bromobenzene and amine concentrations and zero order in base concentration, results which are consistent with deprotonation of the amine by the base occurring only after both

(21) The values given in Table 1 assume that all of the Pd is present as active catalyst. The relative trends in rate constants hold regardless of the actual concentration of active Pd, although the absolute values will be normalized by the fraction of Pd present in the cycle.

(22) The value given in Table 1 for k_1/k_{-1} differs slightly from that found by taking the ratio of the individual values shown in the table because of roundoff error.

(23) The k_{obs} for $[\mathbf{1}] = 0.1$ M at the beginning of the third sequential reaction in Figure 7a may be calculated as 1×10^{-2} s^{-1} (k_{obs} = rate/[Pd]), which is 25 times greater than the k_{obs} measured by Hartwig for oxidative addition at $[\mathbf{1}] = 0.1$ M to $Pd(BINAP)_2$ ($k_{obs} = 4 \times 10^{-4}$ s^{-1}, ref 9).

amine binding and oxidative addition of bromobenzene have taken place. It also precludes the intermediacy of a Pd-alkoxide complex.[1a,1b]

A mechanism in which the amine binds to the catalyst prior to oxidative addition of the aryl bromide is proposed to dominate at [amine]/[bromobenzene] ratios. Oxidative addition of bromobenzene to an (R(R′)NH)Pd(BINAP) complex proceeds more rapidly than direct oxidative addition to the Pd catalyst. The amine also aids in activating the catalyst by facilitating the displacement of dba.

A broader conclusion of these studies addresses the methods by which kinetic data are conventionally obtained. The subtle dependence of the reaction mechanism on relative substrate concentrations raises questions about the value of mechanistic conclusions derived from standard kinetic experiments that typically use concentration ratios distorted from ranges in which synthetic protocols are normally carried out. In addition, the presence of an induction period makes initial rate measurements involving only the first few catalytic turnovers unreliable for providing meaningful kinetic data. Monitoring the reaction progress over time under synthetically relevant conditions provides information that allows mechanistic insight not possible using conventional kinetic measurements and will enable the development of new and more efficient synthetic strategies for practical amination protocols.

Acknowledgment. We thank the National Institutes of Health (GM 45906) for support of this work. We are grateful to Pfizer, Merck, and Bristol-Myers Squibb for additional funds.

JA026885R